Maximum Likelihood Techniques for Joint Segmentation-Classification of Multi-spectral Chromosome Images

Wade C. Schwartzkopf, Alan C. Bovik, *Fellow, IEEE*, and Brian L. Evans, *Senior Member, IEEE*

***Abstract*— Traditional chromosome imaging has been limited to grayscale images, but recently a 5-fluorophore combinatorial labeling technique (M-FISH) was developed wherein each class of chromosomes binds with a different combination of fluorophores. This results in a multi-spectral image, where each class of chromosomes has distinct spectral components. In this paper we develop new methods for automatic chromosome identification by exploiting the multispectral information in M-FISH chromosome images and by jointly performing chromosome segmentation and classification. We (1) develop a maximum likelihood hypothesis test that uses multi-spectral information, together with conventional criteria, to select the best segmentation possibility; (2) use this likelihood function to combine chromosome segmentation and classification into a robust chromosome identification system; and (3) show that the proposed likelihood function can also be used as a reliable indicator of errors in segmentation, errors in classification, and chromosome anomalies, which can be indicators of radiation damage, cancer, and a wide variety of inherited diseases. We show that the proposed multi-spectral joint segmentation-classification method outperforms past grayscale segmentation methods when decomposing touching chromosomes. We also show that it outperforms past M-FISH classification techniques that do not use segmentation information.**

***Index Terms*— Object recognition, image segmentation, partial occlusion, chromosomes, karyotyping**

I. Introduction

Chromosomes are the structures in cells that contain genetic information. When chromosomes are photographed during cell division, the images of these chromosomes contain much information about the health of an individual. In the past it was necessary for laboratory technicians to examine these images visually by lengthy and tedious manual processes of locating, classifying, and evaluating the chromosomes. Since many images often have to be inspected, many attempts have been made to automate these processes; however, automated image chromosome analysis is still an open topic.

In the mid-1990's, a new technique for staining chromosomes was introduced. It produced an image in which each chromosome type appeared as a distinct color [1]. This multi-spectral staining technique made analysis of chromosome images easier, not only for visual inspection of the images by humans, but also for computer analysis of the images. This multispectral staining technique is called *multiplex fluorescence in-situ hybridization*, or *MFISH*. M-FISH uses five color dyes that attach to various chromosomes differently to produce a multi-spectral image, and a

sixth dye that attaches to all chromosomes to produce a grayscale image. Thus it is possible to envision new and improved methods for the location, segmentation and classification of chromosome images by exploiting the color information in M-FISH images.

This paper addresses the topics of segmentation and classification of MFISH chromosome images. It introduces a probabilistic model of M-FISH chromosomes that allows for simultaneous segmentation and classification. The additional information provided by multiple spectra in chromosome images makes it feasible to distinguish chromosomes that overlap and touch within clusters. Thus, we develop a joint segmentation-classification algorithm that optimizes probabilistic information obtained from the multi-spectral chromosome pixels, and enables the decomposition of overlapping and touching chromosomes, and moreover, provides estimates of confidence in the chromosome segmentation-classification.

Specifically, the contributions of this work are as follows:

1) A maximum likelihood (ML) hypothesis test is proposed as a method for selecting the best way to decompose groups of chromosomes that touch and overlap each other. An algorithm is described that efficiently uses this criterion in the multi-dimensional color-space that M-FISH images use. Finally, results of this algorithm are summarized and compared with those of previous methods for chromosome image analysis.

2) This ML test is used to propose a method that combines the task of locating and classifying chromosomes for improved performance in both tasks.

3) The first two contributions in the work are then used to achieve aberration scoring, that is, giving a score to each segment to indicate the likelihood of abnormalities in that image.

II. Background

A. Chromosomes

Chromosomes are the body's information carriers. They are the structures that contain genes, which store in strings of DNA all of the data necessary for an organism's development and maintenance - an intricate schematic for cells and organisms. They contain vast amounts of information; in fact, every cell in a normal human being contains 46 chromosomes, which among them have 6×10^9 bits of information [2].

By examining images of sets of chromosomes in a person, one can collect information about the genetic health of that individual and diagnose certain diseases in that individual. Chromosomes can only be examined visually, however, when they replicate in a process known as mitosis. Under normal circumstances, chromosomes are extremely long and thin and are essentially invisible. However, during the metaphase stage of mitosis, they contract and become much shorter (around 2-10 μm) and wider (around 1-2 μm diameter). At this stage, they can be stained to become visible and can be imaged by a microscope.

B. Karyotyping

Karyotyping is the process of classifying each chromosome in a cell according to a standard nomenclature. In humans, the 46 chromosomes consist of 23 pairs of chromosomes, one of each pair coming from the father and the

Fig. 1. Giemsa banded chromosomes

Fig. 2. Karyotype of Giemsa-banded chromosomes in Fig. 1

other from the mother. Of the 46 chromosomes, there are 22 homologous pairs and two sex chromosomes denoted X and Y (see Figs. 1 and 2). A normal human female has two X chromosomes, while a normal male has an X and a Y chromosome. By convention, the 22 pairs, the X chromosome, and Y chromosome are assigned to 24 distinct classes, where the first 22 classes are numbered in order of decreasing length (that is, class number one is the longest homologous pair of chromosomes), and the last two classes are for the X and Y chromosomes.

There are several features of chromosomes that have traditionally been used for classification. The first and most obvious of these features is size. The second feature traditionally used in karyotyping is the relative centromere position. The centromere is the narrow "neck"-like region in each chromosome. However, by using only the chromosome length and relative position of the centromere, each chromosome cannot be reliably classified into the complete 24 classes of chromosomes, but only one of seven groups known as the Denver classifications [3].

To identify correctly all 24 chromosome types from grayscale images, a banding technique can be used. With proper staining techniques, such as Giemsa banding techniques [4, 5], a unique banding pattern appears on each chromosome type so that all 22 pairs of chromosomes and the X and Y chromosomes could be uniquely identified (Fig. 1). Once all the chromosomes in a cell have been classified, they can be placed into a graphical representation in which they appear in increasing order of their type number. This representation is known as a karyotype (see Fig. 2).

C. Chromosome Abnormalities

Once the chromosomes have been segmented, one can look for abnormalities in them. The most obvious abnormality is an unusual number of chromosomes. Having only one of a type of chromosome is a monosomy, such as Turner's syndrome, in which there is only one X chromosome and no Y. Having three of a type is a trisomy, such as Down's syndrome, in which there are three Type 21 chromosomes.

Other possible abnormalities include deletions. In a deletion, part of a chromosome is lost. An example is William's syndrome, a disorder of the circulatory system. In William's syndrome, the gene that produces a protein that affects elasticity in blood vessels is deleted from a Type 7 chromosome.

There can also be duplications of genetic material within a chromosome and translocations where two chromosomes exchange genetic information. The Philadelphia chromosome results from a translocation in the 9th and 22nd chromosomes. This is often associated with chronic myelogenous leukemia. [6]

There are many other disorders including ring chromosomes, inversions, broken chromosomes, and combinations and variations of the above abnormalities [7]. Detecting these abnormalities is vital because they are reliable indicators of genetic disease and damage and because studying them can lead to new insight about the diseases with which they are correlated. Chromosome abnormalities are particularly useful in cancer diagnosis and research [8].

D. Analysis of Grayscale Chromosome Images

Researchers have been studying how best to use computers to aid in chromosome imaging and analysis for over 30 years [9, 10]. These studies, and object recognition problems in general, have traditionally fallen into one of two categories - segmentation or classification. Although there are a few studies that combine the two categories [11, 12, 13, 14], most fall into one or the other.

1) Segmentation - Segmentation is the process of dividing the image into segments, each of which has some meaning to a human observer. In chromosome analysis, it is desired to segment the image into background and chromosome pixels, and to divide further the chromosome pixels into individual chromosome type pixels. Segmenting a chromosome image into background and chromosome is a fairly straightforward task usually accomplished by thresholding. However, dividing the chromosome pixels into individual chromosomes is quite difficult since chromosomes often touch or overlap. At the point of overlap, pixels may belong to multiple chromosomes.

Stated more formally, the problem of chromosome segmentation is a problem of partitioning the image into minsets [15, 16]. A minset can be defined as

$$M_{\delta_1,\ldots,\delta_{|K|}} \equiv \bigcap_{i=1}^{|K|} \hat{A}_i; \qquad \hat{A}_i \equiv \begin{cases} A_i' & \text{if } \delta_i = 0 \\ A_i & \text{if } \delta_i = 1 \end{cases} \tag{1}$$

where $\{A_i\}_{i\in K}$ is a set of subsets, $|K|$ is the number of these subsets, and $\delta_i \in \{0,1\}$. Thus the set $\{\delta_1,\ldots,\delta_{|K|}\}$ is an index which serves as a binary representation of the minset. Conversely, each subset A_i can be defined by its minsets

$$A_i \equiv \bigcup_{j\in L_i} M_{\delta_1^j,\ldots,\delta_{|K|}^j} \tag{2}$$

where L_i is the set of required minsets. For the case of chromosomes, $M_{0,\ldots,0}$ is defined to be the background; every other minset is defined to be a part unique to one chromosome or common to several chromosomes. In the case of touching chromosomes, each chromosome consists of one minset. In overlapping chromosomes, each chromosome may be composed of several minsets.

Given an image A containing r objects $\{O_i\}_{i=1}^r$, an ideal thresholding operation produces a binary image of objects:

$$O = \bigcup_{i=1}^r O_i \tag{3}$$

and background which is the complement of O

$$B = A - O = O' \tag{4}$$

No segmentation is ideal; the initial segmentation yields a set of q objects $\{O_i^*\}_{i=1}^{q}$ and an estimated background B^*. For each subset O^*, if it can be partitioned into minsets of $\{O_j\}_{j\in\overline{K}_i}$, where $\overline{K}_i$ is given by

$$\overline{K}_i = \left\{ j \middle| O_j \subset O_i^*, 1 \le j \le r \right\} \tag{5}$$

then each object (chromosome) can be written as a union of these minsets.

Agam and Dinstein [16] used minsets to decompose touching and overlapping grayscale chromosomes. In their work, they determined minsets using (rectangular) shape-based hypothesis testing to choose cut points for dividing clusters of chromosomes. Their method was successful in many cases but limited to grayscale chromosome images.

A wide variety of other approaches have also been proposed. A split-and-merge technique [17] uses a "watershed" [18] method to oversegment the image. This is similar to region-growing [19, 20] methods, which grow seed segments until they meet, combining segments only if they satisfy a certain criteria, such as convexity. However, these methods are only useful for decomposing touching chromosomes and do not handle overlaps.

Fuzzy set theory [21] has also been applied to chromosome segmentation. Fuzzy binary relations are defined on the boundary points of high curvature, and fuzzy subsets are defined over the points that make up the boundaries. This method works for simple cases but fails when the chromosomes are bent or clustered [16].

"Valley searching" attempts to find "valleys" of gray values representing separations of chromosomes. Vossepoel [2] defines a set of rules by which to find candidate cut points and then to link points with a minimum-cost algorithm. This method often works well at finding accurate boundaries, but it also does not handle overlaps.

A model-based method was described in [22] that characterized different types of boundary features highly correlated with touches and overlaps. This method showed success in recognizing clusters but had a relatively high failure rate for finding plausible separation paths.

Ji [23] used the concepts of skeletons [24] and convex hulls to decompose overlaps. This work has shown some of the most successful results in the literature, but still is limited since it only uses grayscale and geometric information.

2) Classification - Classification usually follows segmentation in chromosome image analysis. Once segmented and classified, it is simple to arrange the chromosomes into a karyotype (see Fig. 2) for examination. After segmentation, chromosomes have a number of features, including length, centromere index, and banding pattern, that can be used to classify them. Length is simple to measure for properly segmented chromosomes, but centromeres are subtle and sometimes difficult to locate. Length and centromere index by themselves cannot be used to classify chromosomes reliably into their 24 classes. Hence the banding pattern has been a popular feature for manual and automated chromosome classification. However, banding patterns are often difficult to extract automatically. Often a medial axis transform [25] is performed to measure a density profile by integrating the intensities along sections perpendicular to the medial axis. However, bent chromosomes can be difficult to straighten in cases with sharp bends. Further, the banding patterns of overlapped chromosomes are often obscured.

Several transforms have been proposed for representing chromosome banding patterns. Fourier descriptors have been used as global descriptors of the chromosome's density profile, and the first eight components of the Fourier transform were found to be most useful for discrimination [26]. Another transform proposed in [27] describes a set of weighted density distribution functions which serve as a set of basis functions. Each chromosomes's density profile was correlated with these functions, and the correlations served as a representation of that chromosome, rather than the profile itself. This is one of the most commonly used technique for banding pattern classification.

Laplace local band descriptors [28] have been used to extract only the most dominant bands, since these bands were believed to be the most significant for classification. A 2-D Laplacian filter and a set of thresholds were used to determine the size and position of the larger, darker bands on the chromosome. Features from these bands, such as width, position, and average density, are then fed to a classifier.

Markov chains [29] have also been used to represent the banding patterns of chromosomes. In this approach the density profile is quantized and represented as a chain of symbols. A set of density profiles from the same class are used by an inference technique to build a constrained-first order Markov chain representation. When a chromosome is classified, its profile is assigned to the class represented by the Markov chain most likely to produce that profile.

A number of different classifiers have been used as well. These include neural networks [30, 31]. In one neural network implementation [32], a multi-layer perceptron neural network was used. Chromosome length, centromere index, and 15 points from a 64-element density profile were used as features.

Homologue matching [33, 34] uses two criteria for classifying chromosomes. For a chromosome to be classified as a certain class, it first must be similar to a typical chromosome of that class. Second, it must be similar to the other chromosomes of that class in the same image. This is useful for detecting chromosome abnormalities.

Other approaches include fuzzy classifiers [35] whose output is a numerical measure of similarity to a known class and several other statistical methods. A good review of these methods is given in [36]. While notable success has been achieved with these methods, they all suffer from the same drawback, that they rely on features, such as centromere position and banding pattern, which can be difficult to measure and depend on segmentation accuracy.

3) Joint Segmentation-Classification Methods - Traditional image analysis methods have viewed segmentation and classification as separate processes. However, the two processes are closely related. Each can be improved with information that the other provides. In the case of chromosome segmentation, this has been realized and suggested before. Ji [37, pp. 188-189] realized that classification would benefit from correct segmentation information, and that segmentation often needs data from classification as well; he suggested a system of feedback. Agam and Dinstein [16] also realized this and suggested combining the steps for more accurate identification. Both recognized the potential usefulness of combining segmentation and classification, but provided no method to accomplish it.

Martin [13] combined segmentation and classification for a different problem: optical character recognition. More recently credibility networks were proposed as a framework for joint segmentation and classification [14]. Both of these attempts show promise, but neither is easily extensible to objects without definite shapes, such as chromosomes. An attempt at combining classification and segmentation for chromosome images was made in [12], which used classification-driven segmentation to handle chromosome cluster decomposition. Positive results were

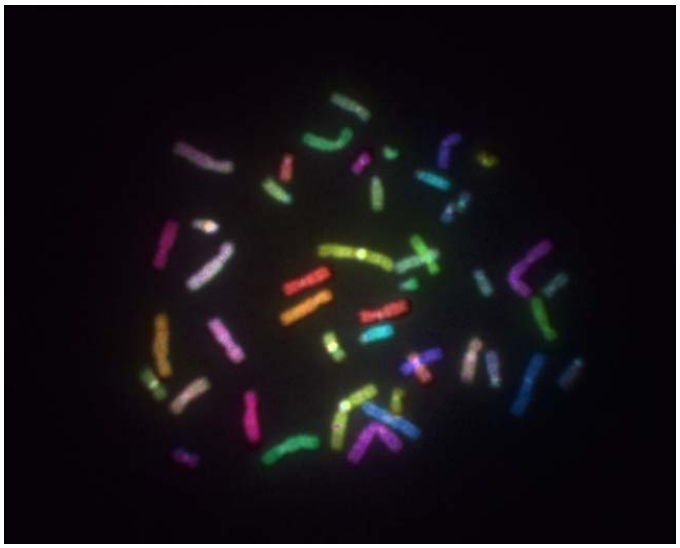

Fig. 3. M-FISH Image

TABLE I

SEGMENTATION AND CLASSIFICATION METHOD COMPARISON

Method	Segmentation Accuracy		Classification Rate	Joint Segmentatio-Classifcation
	Touch	Occlusion		
Vossepoel [2]	Medium	n/a	n/a	no
Lerner [12, 32]	High	n/a	84%	yes
Agam [16]	High	High	n/a	no
Wu [22]	Low	Low	n/a	no
Li [23, 37]	High	High	n/a	no
Granum [27]	n/a	n/a	90%	no
Groen [28]	n/a	n/a	89%	no
Stanley [34]	n/a	n/a	80%	no

achieved. However, it was limited to grayscale chromosome images and did not consider overlaps. In addition, it made no provisions for images of multiple clusters or clusters of more than two chromosomes.

4) Comparison - Table I shows a comparison of several different segmentation and classification algorithms. This table must be viewed with a bit of caution. *It is difficult to compare methods directly since published methods rarely use rates directly comparable with other work.* In segmentation, some proposed methods measure touch and decomposition and overlap decomposition separately; others do not distinguish between the two. Some use full real-world images of chromosomes, while others were only tested on pairs of overlapping or touching chromosomes. Also, many published segmentation rates are run on different sets of data. There are at least five grayscale chromosome datasets used in the literature: Copenhagen [28, 36], Edinburgh [32, 36], Philadelphia [36], Delft [28], and Soroka5 [32]. Because of difficulties in comparing methods directly, we have quantized the published segmentation accuracy rates of the methods to low (<70%), medium (70-80%), and high (>80%).

Classification rates are also difficult to compare directly. Some classify only within a set of chromosome types rather than all 24 types. Some assume perfect segmentation; others do not. In addition, some classification methods propose new feature representations, while others propose new classifiers; it is difficult to directly compare the merit of two features if they are not used with the same classifier. In spite of these difficulties, we include Table I as a rough comparison of methods that have published some segmentation and/or classification accuracy rates.

E. M-FISH Images

A new way to acquire chromosome images derives from the invention of chromosome painting [38] and combinatorial [39] and ratio labeling [40]. These techniques make use of fluorophores (dyes) that attach to a single type of chromosome, parts of chromosomes, or specific sequences of DNA. Using these techniques, it is possible to create a combination of fluorophores such that each class of chromosomes absorbs a different combination of these fluorophores [1, 41, 42]. Since each fluorophore has a different emission spectrum, each chromosome class appears

as a different color visually distinguishable from all other classes without the aid of banding patterns. An image of each fluorophore can be obtained by employing appropriate optical filters. With 5 fluorophores, a multi-spectral image is obtained where each pixel is represented as a 5-D vector, with each element in the vector representing the magnitude of one fluorophore at that point. Instead of the grayscale image that was obtained in traditional chromosome imaging techniques, a multi-spectral image is now available in which the spectral composition at each point reveals the combination of fluorophores and, thus, the chromosomal origin of the matter at that point. Using this combinatorial labeling, known as M-FISH, it is possible to determine the most likely chromosomal origin at every point in the image [43]. An example of an M-FISH image is shown in Fig. 3.

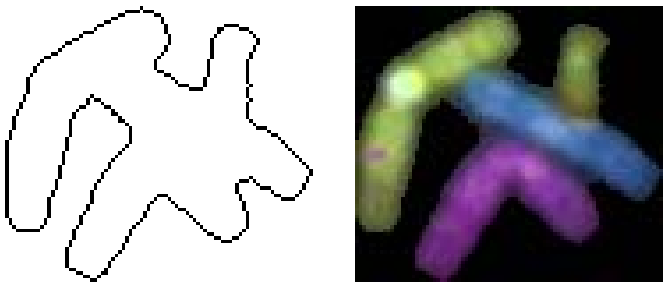

(a) Boundary of cluster (b) Multi-spectral information in cluster

Fig. 4. Comparison of two types of cluster information

Such an imaging technique has a few obvious advantages. First, the task of chromosome classification is greatly simplified. Instead of having to estimate features such as centromere positions and banding patterns, which may be difficult to measure, one only has to look at the spectral information within that chromosome. The second advantage is that it is possible to detect smaller translocations and rearrangements than were discernible with banding patterns only [44]. Small translocations are easily noticed as a single chromosome with two different colors in it.

With M-FISH images, an entirely new source of information is available for segmentation as well. If one observes the example in Fig. 4, it is not immediately clear, by looking only at the boundary of the cluster, what the proper segmentation of the cluster is. It is not apparent, even to many human observers, whether there is an overlap involved or even how many chromosomes are included in this cluster. However, by looking at the M-FISH multi-spectral information, a human observer would very easily be able to determine what the proper segmentation should be since each chromosome has its own color.

Several sets of fluorophores are commonly used for M-FISH imaging. In all these sets, one fluorophore, DAPI (4',6-Diamidino-2-phenylindole), which attaches to DNA and thus labels all chromosomes, is typically used to generate a traditional grayscale image of the chromosomes. Five additional fluorophores are used to distinguish chromosome class. A Bayesian classifier was proposed in [43] that can be trained on each set of images to compensate for different fluorophore characteristics that may occur in each set. The method calculates the maximum *a posteriori* probability (MAP) of a pixel belonging to each class, and the most likely class is selected. This classifier has proven to be very successful, and the pixel classifier used here is based on this work (see Section III.B).

During pixel classification, special care must be taken with areas of overlap. With M-FISH, the chromosomes are illuminated from above and viewed from above, so the major contribution for a pixel in an area of overlap will come from the top chromosome. However, in practice, the chromosomes are somewhat transparent, so that pixel will include information from both chromosomes. This could lead to a pixel being classified as the same type as the top chromosome, the same type as the bottom chromosome, or neither.

F. Analysis of M-FISH Images

To date there is little work on image analysis of M-FISH chromosomes images. An entropy criterion for segmenting class maps of chromosome cluster was explored in [45]. This was an early, primitive attempt at using multi-spectral information to segment chromosome images. Some success was shown, but the success of the method was very sensitive to its parameters, and it was not robust over a wide variety of images. Furthermore, this method only performed chromosome segmentation. No chromosome classification method was proposed, and thus classification information could not be used to aid in segmentation. The entropy approach was extended to use entropy estimation for application directly to M-FISH data [46], but it achieved little success.

The next step in the evolution of chromosome imaging is the application of image analysis and pattern recognition techniques to multi-spectral M-FISH images. These images provide significantly more information than grayscale chromosome images and promise significant improvements in the accuracy of chromosome identification, classification, and anomaly detection. While 24-color chromosome labeling [1] has greatly simplified the classification of chromosomes, it is not immediately clear what is the best way to use multi-spectral methods to segment the image and decompose touching and overlapping chromosomes.

Recall that in grayscale images, binary segmentation usually results in as many or fewer objects than chromosomes. However, in the multi-spectral images, an initial segmentation may break the image into *at least* as many objects as there are chromosomes in the image. That is, $q \leq r$ in the minset notation. For example, it is likely that two overlapping chromosomes would segment into three parts. While chromosome segmentation in the grayscale case was a "splitting" problem, it becomes a "merging" problem in the multi-spectral case.

Any useful multi-spectral segmentation technique must also resolve touching and overlapping chromosomes without losing the ability to detect translocations and rearrangements. A useful criterion must be found for distinguishing between translocations, in which a chromosome may be made up of two colors, and touching (or overlapping) chromosomes, in which two separate chromosomes of different colors appear to be connected.

M-FISH eliminates many of the prior difficulties encountered in chromosome classification. No longer are centromere location, banding pattern, and other complicated, difficult to measure, features necessary to determine a chromosome's class since color alone is theoretically sufficient to determine the class. Since each pixel can be classified individually, each chromosome is assigned to the class to which most of its pixels have been classified.

Yet another benefit for M-FISH is that classification can be performed independently of segmentation. Grayscale methods were often forced to perform segmentation followed by classification, since the grayscale classification features could only be measured on a segmented chromosome. With M-FISH images, it is possible to reliably estimate what class a pixel belongs to before it is known what segment it belongs to. This is very useful, as seen in Section III, since this classification information can be used to attain more accurate segmentation; this more accurate segmentation will, in turn, yield more accurate classification.

III. Maximum Likelihood Algorithm for Joint Segmentation-Classification

We now formulate the chromosome segmentation-classification problem as an ML hypothesis test. We will then use the formulation to segment and classify multi-spectral chromosome images efficiently.

A. Problem Formulation

We define C_i as the set of all pixels belonging to class i. Since there are 24 classes of chromosomes, each non-background pixel may be classified as one of 24 classes. We do not explicitly handle background pixels since we assume that background/foreground segmentation is performed as a preprocessing step before any other segmentation is carried out.

A_i^n denotes the set of pixels belonging to the n^{th} chromosome of class i in a single image, or in a set of images. Within any set of images, several chromosomes may belong to the same class: $A_i^n \subseteq C_i$. $\left|A_i^n\right|$ denotes the cardinality of the set, which is the number of pixels in the chromosome.

We want to find the sets A_i^n that represent the chromosomes that need to be segmented and classified. In general, given a likelihood function, or a measure of the probability that an arbitrary segmented object is a chromosome A_i^n, the segmentation-classification problem reduces to choosing the segmented objects and corresponding classes to maximize the likelihood function. We also need a mechanism for generating candidate chromosomes for evaluation using the ML hypothesis test. This is the subject of Section IV.

Thus the joint chromosome segmentation-classification problem is composed of three steps:

1) Design a likelihood function to evaluate the likelihood that a candidate chromosome is of a certain class

2) Generate sets of candidate chromosome segmentations, and

3) Use the ML test to select both the best set of candidate chromosomes and their classes.

The joint segmentation and classification method developed herein for multi-spectral images also employs a form of classification-driven segmentation [12]. A set of likelihood functions is used to accomplish segmentation and classification simultaneously. It does not employ segmentation-classification feedback and hence does not suffer from error propagation due to outliers in segmentation or classification. Further, the probabilistic modeling results in an intuitive and extensible framework for the segmentation and classification of chromosomes.

B. Proposed Likelihood Function

The proposed likelihood function $L(\cdot)$ is a product of three components: two likelihood functions $L_{multi}(\cdot)$ and $L_{size}(\cdot)$ and a weighting function $w(\cdot)$ that accounts for overlaps and improves segmentation accuracy, where $0 < w(\cdot) \le 1$. The likelihood function $L_{multi}(\cdot)$ uses multi-spectral information, while $L_{size}(\cdot)$ uses information on the relative chromosome size. $L(\cdot)$ is a function of a possible chromosome segmentation and a possible class. Thus $L(\cdot)$

incorporates information central to both segmentation and classification. Clearly, $0 \le L(\cdot) \le 1$. In the following, a possible segmentation of a single chromosome is referred to as a *candidate chromosome.*

Definition 1. Given a candidate chromosome A', the likelihood that A' belongs to the class i, due to the multi-spectral data in its pixels, is given by $L_{multi}(A', i) = \mathrm{E}\left[p(\mathbf{m} \in C_i \,|\, \mathbf{x}(\mathbf{m})) \,\middle|\, \mathbf{m} \in A'\right]$, where $\mathbf{m}$ denotes a pixel, $\mathbf{x}(\mathbf{m})$ is the multi-spectral data at that pixel, and E is the expectation operator.

The likelihood function $L_{multi}(\cdot)$ averages the probabilities that each pixel in A' belongs to class i. By Bayes' theorem:

$$P(C_i|\mathbf{x}) = \frac{P(\mathbf{x}|C_i)P(C_i)}{P(\mathbf{x})} \tag{6}$$

In (6), the terms $P(\mathbf{x}|C_i)$, $P(\mathbf{x})$, and $P(C_i)$ were estimated from training data by fitting a Gaussian Mixture Model to determine the conditional distributions [43]. These terms can be calculated as follows

$$P(\mathbf{x}|C_i) = G(\mathbf{x}, \boldsymbol{\mu}_{1,i}, \boldsymbol{\Sigma}_{1,i}) \tag{7}$$

$$P(\mathbf{x}) = \sum_i P(\mathbf{x}|C_i) \tag{8}$$

$$P(C_i) = \frac{\sum_n \left|A_i^n\right|}{\sum_j \sum_n \left|A_j^n\right|} \tag{9}$$

where $G(\cdot,\cdot,\cdot)$ is a Gaussian probability density function. The means and covariance matrices ($\boldsymbol{\mu}_{1,i}$ and $\boldsymbol{\Sigma}_{1,i}$, respectively) are computed using ML parameter estimation [47] on the training set. The subscript 1 in $\boldsymbol{\mu}_{1,i}$ and $\boldsymbol{\Sigma}_{1,i}$ is used to distinguish these means and variances from those in Definition 2, and the subscript i denotes class. In the case of M-FISH images, training should be applied to each batch, or group of images of similar characteristics, since each batch has its own set of dye characteristics. Training can be accomplished by using a few images that have been hand segmented. The prior class probabilities, $P(C_i)$, also must be computed by training on a set of data. Then $P(C_i)$ is calculated as the percentage of all chromosome pixels in the training data that belong to class C_i. However, since relative chromosome size does not vary from image to image, this does not require retraining for each new data set.

As a complement to multi-spectral information, we also define another likelihood measure to avoid the erroneous segmentation of chromosomes into small segments of locally similar pixels.

Definition 2. Given a candidate chromosome A', the likelihood that A' belongs to the class i, due to its size, is

$$L_{size}(A', i) = G\left(\frac{|A'|}{y}, \mu_{2,i}, \sigma_{2,i}\right) \text{ where } y = \sum_n \sum_j \left|A_j^n\right|.$$

This second likelihood function is a function of object size. When the size of the candidate chromosome A' is equal to $\mu_{2,i}$, the mean size of class i, then the likelihood L_{size} value will be greatest. The size variance of each class i is denoted by $\sigma_{2,i}$.

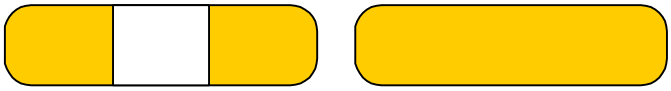

(a) Incorrectly segmented b) Correctly segmented

Fig. 5. Shaded areas represent two possible segmentations, A' of a single chromosome. The function w(A') gives more weight to case b).

The size of a chromosome is its relative size, or the percentage of total chromosome area in the image that a chromosome covers. This makes the likelihood function scale invariant. Hence, while a change in microscope magnification might produce larger chromosomes, it would result in the same value for the likelihood function due to the normalization of the chromosome size by y, which is the total chromosome area within the image.

Using this second likelihood function accomplishes several things. First it adds a second, completely different source of information for classifying chromosomes. As mentioned in Section II.B, size is insufficient to classify a chromosome reliably into one of the 24 classes. However, it complements the first likelihood function.

The likelihood function L_{size} also distinguishes fragments from whole chromosomes. Without it, an oversegmented chromosome would be no less likely than a correctly segmented chromosome, since both would have the same multi-spectral information, and thus the same value for L_{multi}. Moreover, a broken chromosome or a section of a translocation would be indistinguishable from a normal chromosome. In addition, a likelihood function based on size is very useful for detecting clusters of chromosomes, since a cluster of chromosomes will generally be larger than any of the mean sizes of the classes given high likelihood values by L_{multi}.

In addition to these two likelihood functions, one final component is defined to model overlaps.

Definition 3. Given a candidate chromosome *A'*, the certainty, *w*(*A'*) of the likelihood functions in Definitions 1 and 2 is defined to be the percentage of visible, or non-overlapped, pixels in the candidate chromosome *A'*.

Chromosomes that are overlapped by other chromosomes are less certain than chromosomes that are completely visible, since the function has less information about them. Thus, *w* acts as a weighting function of the overall likelihood function. This may be viewed as an adjustment to take into account overlapping chromosomes, since the weighting function returns a value of unity when there is no possible overlap.

Incorporating *w* also improves segmentation accuracy by preventing segments from being omitted from the middle of chromosomes. Fig. 5 illustrates this possibility. Since *A'* in Fig. 5 (a) consists of two connected components, the middle (white) portion of the chromosome is assumed to be an area of overlap; the size of both segmentations, and thus, L_{size} is calculated to be the same. Without weighting, if L_{multi} were the same for both segmentations, then L would be as well, although the correct segmentation, Fig. 5 (b), should receive a higher likelihood value.

Here *A'* is the non-overlapped area of the candidate chromosome. The overlapped area is estimated as the area between the connected components of A' (see Fig. 6). If A' contains only one connected component, then it is assumed that the candidate chromosome is not overlapped, and hence *w*(*A'*) = 1.

The area of overlap is estimated as follows: First the set of all pixels in the two segments under evaluation, that border the rest of the connected component, or chromosome cluster, are found. Then a line is drawn from each pixel in the first set of border pixels to every pixel in the second set of border pixels. This does not guarantee a continuous area without gaps, so the process is finished by filling holes in the new segment created from the lines drawn. The new segment then estimates the overlapped area of the chromosome. This estimate is needed to calculate the chromosome size in L_{size} and the percentage of visible pixels in *w*.

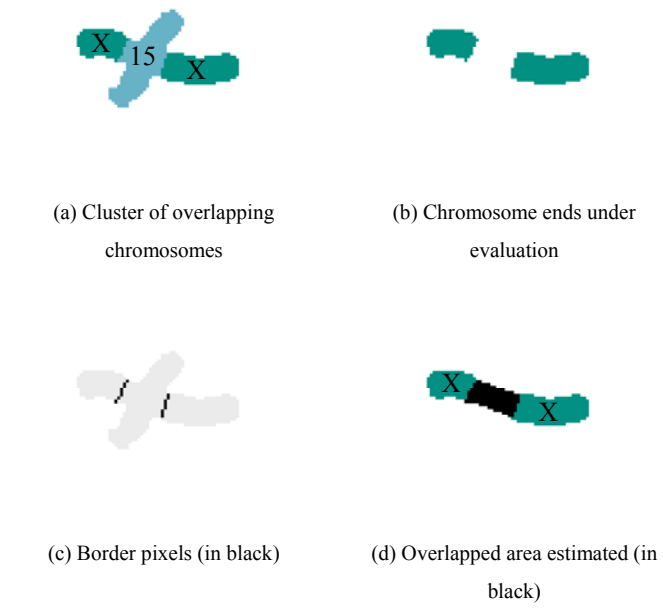

(a) Cluster of overlapping chromosomes

(b) Chromosome ends under evaluation

(c) Border pixels (in black)

(d) Overlapped area estimated (in black)

Fig. 6. Calculating the area of overlap.

Fig. 6 depicts estimation of the overlapped area with an actual chromosome. Here a type 15 chromosome is overlapping an X chromosome. Fig. 6(b) shows the ends of the X chromosome to be evaluated. To calculate the area of overlap, the pixels that border the rest of the cluster (Fig. 6(c)) are found and connected. This gives the estimate of the overlapped area in Fig. 6(d) - 136 pixels. The visible ends of the X chromosome have an area of 377 pixels, so if A' is the area shown in Fig. 6(b), the weighting function is calculated as follows:

$$w(A') = \frac{\text{visible area}}{\text{estimated total area}} = \frac{377}{377+136} = 0.74 .$$

Definition 4. Given a candidate chromosome A', the overall likelihood that A' belongs to the class i is $L(A',i) = L_{multi}(A',i)L_{size}(A',i)w(A')$.

Classification is accomplished by using the ML hypothesis on the candidate chromosome *A'*. The most likely class is given by the value of i maximizing $L(A',i)$ for a given A'. Segmentation is accomplished using the ML hypothesis on a set of possible segmentations. Classification maximizes $L(A',i)$ over i, and segmentation maximizes $L(A',i)$ over A'. By maximizing both A' and i over $L(A',i)$, segmentation and classification are simultaneously accomplished:

$$\arg\max_{A',i} L(A',i) \tag{10}$$

Here ML classification is essentially equivalent to maximum *a posteriori* (MAP) classification, since the prior probabilities for each class are mostly equal. For any candidate chromosome, all classes are equiprobable since each class of chromosome occurs with the same frequency (2) in most images. The exception is the X and Y chromosomes - a normal image will have a pair of X's and no Y's (female), or one of each (male). However, since this exception

(a) Color representation of M-FISH cluster

(b) Segmented cluster

Fig. 7. Typical chromosome cluster in M-FISH image segmented with cutlines. Yellow crosses mark cut points. In this case, lines closely approximate the boundaries between chromosomes.

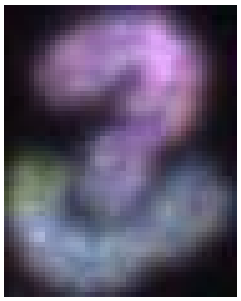

Fig. 8. Cluster that cannot be split with a cutline.

concerns only 2 of the 24 classes, we have chosen to ignore it and to approximate the MAP classifier via ML. The other possibility would be to assume that male and female karyotypes were equally as likely so that there would be 1 Y chromosome and 3 X chromosomes per 2 images, or 92 chromosomes. This would give priors of 1/92 for the Y class, and 3/92 for the X class.

IV. M-FISH Classification-Segmentation Implementation

It is important to contrast our work with traditional chromosome segmentation methods. Traditional methods begin with clusters of chromosomes and attempt to divide them into individual chromosomes by choosing cut points on the boundary of the cluster, which are the points at which the boundaries of the two different chromosomes meet. Given two touching chromosomes, two points must be found that define a line separating the chromosomes. Given two overlapping chromosomes, four cut points must be found that create a polygon representing the area of overlap. Once the proper cut points are discovered, the touching or overlapping chromosomes are decomposed by straight cut lines between the points [16] or best fit cubic curves [23] (See Fig. 7). Whereas traditional approaches often begin with undersegmented objects, we begin by *oversegmenting* chromosomes, and then merge the segments. These segments are derived from multi-spectral information and pixel classification. The segments, or combinations of them, are often able to represent the intricate boundaries between chromosomes more accurately than a single cutline (Fig. 8).

Traditional chromosome segmentation methods use shape information from the boundary of the chromosomes as a criterion for selecting possible segmentations and for detecting clusters. Methods that search for branches in skeletons [23] have been used to detect clusters. Many algorithms have examined cluster boundary shape to select cut points [16, 22, 23]. Occasionally, grayscale information from inside the chromosome clusters has been used, e.g., "valley searching" [2] whereby low gray-value valleys running through the cluster are used to locate separation between the chromosomes. We instead use the multi-spectral information available in M-FISH as a criterion for selecting from a set of segmentation possibilities, by incorporating it into a likelihood function to evaluate these possibilities. We select the most likely via an ML hypothesis test.

A. Determination of Candidate Chromosomes

Section III-B poses the segmentation-classification problem as maximizing the likelihood function $L(A', i)$. Since there are only 24 possible classes for a chromosome, it is simple to do an exhaustive search over all possible values of i for any particular candidate chromosome A'. However, there is an extremely large number of possible segmentations for A', so this formulation is only useful if one could somehow first develop a reasonably limited set of candidate chromosomes from which to choose. We now describe how these candidate chromosomes are generated.

Many previous chromosome segmentation methods [37] begin with a background/foreground separation step, such as thresholding. This segments all the single chromosomes with no touches or overlaps. By contrast, we focus only on decomposing clusters of overlapping and touching chromosomes. Of course, erroneous background/foreground segmentation may lead to erroneous cluster decomposition; however, there has already been a great amount of work on this problem, so we refer the reader to [48] for a review of some of the many techniques available. In this work, we assume that background/foreground segmentation has been performed ideally or at least close to ideally.

We perform connected component analysis to parse the image into single chromosomes and clusters of touching and overlapping chromosomes. The result of this processing is a set of r connected components, or objects, $O_1^* \ldots O_r^*$. At this stage, each object O_i^* is probed using the likelihood function developed in Section III.B. If O_i^* were a complete chromosome, evaluation of the likelihood function for the correct class will result in a large value; if O_i^* were composed of several touching and/or overlapping chromosomes, a small likelihood value will result. If O_i^* were a single abnormal chromosome, then it would also result in a small likelihood value. An empirically determined likelihood threshold, T_1, is used to determine whether the connected component O_i^* is a single, normal chromosome. If the ML function evaluated on O_i^* exceeds T_1 for any class, then processing is terminated because the component has been both segmented and classified with a high likelihood value.

If the likelihood function falls below T_1, then the connected component could either be a cluster of touching and overlapping chromosomes or an abnormal chromosome, such as a broken chromosome or translocation, or a combination of these. All of these cases are handled in a unified manner using pixel classification and post-processing of the classification map. The post-processing step reduces noise in the pixel classification, improves computational efficiency, and increases the segmentation-classification accuracy. The objective is to partition the connected component O_b^* into mutually disjoint sets $O_{b,1}^* \ldots O_{b,q}^*$, where b indexes a connected component with likelihood function below T_1 for all classes. Since the sets completely make up O_b^*,

$$O_b^* = \bigcup_{j=1}^{q} O_{b,j}^* \tag{11}$$

and since the sets are mutually disjoint

$$\bigcap_{j=1}^{q} O_{b,j}^{*} = \varnothing \; \forall b \tag{12}$$

We now describe the details of this partitioning process, and then explain how the sections are re-merged.

1) Pixel Classification and Post-processing - Each connected component O_b is first processed by a pixel classifier using the MAP $p(C_i|\mathbf{x})$ discussed in Section III-B. Since pixel classification is a noisy process, some isolated pixels and small segments are misclassified in this step. To reduce noise, we filter the class map using a non-linear majority filter. The majority filter is used since it removes small segments, but maintains the shape and position of large-scale edges. A majority filter uses a moving window H. The image is scanned in raster order, and the class at the center pixel location is replaced by the majority class within the spatial extent of the window:

$$y(\mathbf{m}) = \underset{\mathbf{k}\in H,(\mathbf{m}-\mathbf{k})\in\{O_i^*\}}{\text{maj}} \{x(\mathbf{m}-\mathbf{k})\} \tag{13}$$

Here, x is the input class map, y is the output class map, and *maj* denotes the majority operation. Notice that only object pixels are used for calculating the majority, not background pixels. We use a fairly large window $H = \{(-8,-8),(-8,-7),\ldots,(8,8)\}$ - a 17 × 17 square applied to 517 × 645 images - large enough to remove most of the noise; but not be so large that it removes small chromosomes. This window is about the same size as the smallest chromosome in an average image – in fact, not large enough to filter out even the smallest chromosome in the ADIR M-FISH chromosome image database (Section V.A). Another possibility is to vary the window size by adaptively selecting a window smaller than the expected size of the smallest chromosome in a given image. It should be noted that a large majority filter might also remove small translocations. This is acceptable though, since it is not necessary to split translocations into two segments; instead, objects are identified as translocations by low likelihood value.

We follow majority filtering by reclassifying small segments to the most likely class of one of their neighboring segments. This eliminates any remaining small segments. If S_j is the set of pixels in the segment under examination, define S_j to be a small segment if $|S_j| < T_2$. For each small segment, the set of classes of the adjacent segments is denoted D_{S_j}. Two segments, S_{j_1} and S_{j_2}, are *adjacent* if

$$\exists \mathbf{x}(\mathbf{m}) \in S_{j_2} \text{ such that } \mathbf{x}(\mathbf{m}-\nabla) \in S_{j_1} \tag{14}$$

where ∇ is the four-connected set $\{(0,1),(1,0),(0,-1),(-1,0)\}$. The most likely class, $\hat{i}$, is determined by selecting the most likely class for S_j from among only the classes of its neighboring segments, D_{S_j}

$$\hat{i} = \max_{i\in D_{s_i}} L_1(S_j, i). \tag{15}$$

Figure 9 depicts small segment reclassification; Fig. 9(a) shows a class map of classified pixels, where color denotes class. It includes two large segments, labeled 1 and 2. One small segment of only two pixels, labeled 3, remains even after majority filtering. To remove this small segment, it is reclassified to the most likely class of one of

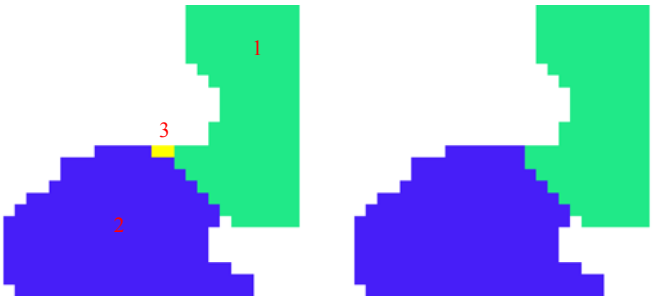

(a) Small segment is #3 (b) Reclassified as neighbor class

Fig. 9. Small segment reclassification

(a) Overlapped chromosome: two class 5 segments (b) Two whole chromosomes: two class 6 segments

Fig. 10. Ambiguity of similarly classified segments

its neighbors, so that it becomes the same class as one of these segments (Fig. 9(b)). In the example, the small segment is reclassified to the same class as segment 1, so both segments are denoted in blue.

The steps of pixel classification, majority filtering, and reclassification generally yield oversegmented chromosomes - more segments result than there are chromosomes. In the next section, it is shown how these segments are rejoined to create candidate chromosomes. The resulting segments $\{S_j\}$, after majority filtering and reclassification, are equivalent to the partition used in Agam and Dinstein's minset representation of the chromosome segmentation problem [16]. The chromosomes can be then formed as minsets of this partition. Next, we describe how to choose which set of segments to represent each chromosome.

2) Rejoining of Segments into Candidate Chromosomes - The above steps typically result in oversegmented chromosomes; that is, there is often more than one segment for each chromosome. This is because there are often misclassified segments. In addition, even if pixel classification were performed perfectly, one would need some mechanism to distinguish between which pairs of similarly classified segments represent the ends of one overlapped chromosome and which represent two whole chromosomes within a single cluster. Figure 10 illustrates these two possibilities. It shows two clusters of classified segments: Fig. 10(a) shows a cluster with two segments classified as class 5; they are two ends of an overlapped chromosome and should be joined together since they are part of the same chromosome. Fig. 10(b) shows two segments classified as class 6. In this case, the two segments are two complete chromosomes and should be recognized as separate.

In the rejoining process all possible pairs of segments are considered as candidate chromosomes; the likelihood function L is computed for each pair. The pair that results in the largest likelihood value is combined into a single segment, if the conjoint likelihood value exceeds the geometric mean of their individual likelihood values. After the pair is rejoined to make a new segment, all possible pairs of the new set of segments are evaluated to find the combination which results in the greatest likelihood value. This process is repeated until no more pairs can be found whose combination results in a greater likelihood value that the geometric mean of the two original likelihood values in the pair.

The first two pairs are selected as follows:

$$(\tilde{j},\tilde{k}) = \arg\max_{j,k,j\neq k} L\left(S_j^1 \bigcup S_k^1\right) \tag{16}$$

The rejoining of two segments is given as

$$S_f^{l+1} = S_{\tilde{j}}^{l} \bigcup S_{\hat{k}}^{l} \tag{17}$$

where f is an index into a reordered sequence of segments. We repeat this rejoining as long as

$$\max_i \sqrt{L\left(S_{\tilde{j}}^{l}\right) L\left(S_{\tilde{k}}^{l}\right)} < \max_i L\left(S_f^{l+1}\right) \tag{18}$$

Since we want to encourage recombining tiny segments which result in a near zero likelihood value, the geometric mean is preferred to the arithmetic mean.

When no more pairs can be found to be suitable for recombination, the segmentation-classification is complete, and the chromosome segmentation-classification estimates are labeled. Note that abnormal and incorrectly segmented chromosomes result in low likelihood values and thus can be identified and flagged.

Figure 11 shows an example of segment rejoining; Fig. 11(a) shows the segments left after pixel classification, majority filtering, and small segment reclassification. Two segments in the Class 6 chromosome have been misclassified as Class 14. The two Class 6 segments were joined first, then the lower Class 14 segment; and finally, the upper Class 14 was joined with the new segment made of the original two Class 6 segments and the lower Class 14. The new large segment was classified as a Class 6 chromosome. Joining the Class 6 and the Class 11 chromosomes did not result in an increase in the likelihood value, so rejoining was stopped. The final result is shown in Fig. 11(b). A flowchart of the algorithm is given in Fig. 12.

V. Results

A. M-FISH Chromosome Image Database

The algorithm was tested on the ADIR M-FISH chromosome image database [49] of 200 multi-spectral images of dimension 517 × 645. Each pixel contains a 6-element vector: 5 multi-spectral channels plus the grayscale DAPI channel, as discussed in Section II-E. This database is a representative set of M-FISH images with a wide variety of image types and from a variety of dye sets. It includes very simple images with no touches and overlaps between chromosomes as well as difficult-to-segment images with many touches and overlaps. It includes crisp, clear images as well as somewhat blurry ones. It includes well-spread chromosomes and tightly packed chromosomes. It includes chromosomes at different stages of mitosis. It includes normal male and female karyotypes, sets with simple translocations, and "extreme" cases (labeled karyotype code 'EX') with many abnormal chromosomes.

A nomenclature is used on the images to easily identify karyotype and set. The first character represents the probe set. The next two characters represent slide number. The next two characters are the number of the image on the slide. The final two characters represent the karyotype code. Therefore, if image number 12 from slide 98 (using ASI probes) were from a normal female, its file name would be A9812XX. The dataset is publicly available and can be used by anyone for comparing M-FISH segmentation results. The dataset also includes an ISCN designation of the karyotype and *a hand-segmented "ground truth" image* for each M-FISH image (marked with a 'K'), so that segmentation results can be easily checked for accuracy.

(a) Segments after pixel classification and post-processing (b) Final segments after rejoining

Fig. 11. Rejoining of segments to make chromosomes

We ran the algorithm on every image other than the "extreme" cases. Each image, together with segmentation results compared to the ground truth ('K') images were manually analyzed and recorded. Since few segmentations will be pixel-for-pixel identical with the stored K image, this task is somewhat subjective. In all comparisons, we were somewhat lenient with both algorithms and accepted any segmentation that varies only slightly from the K image in the database. The results are presented in the following sections.

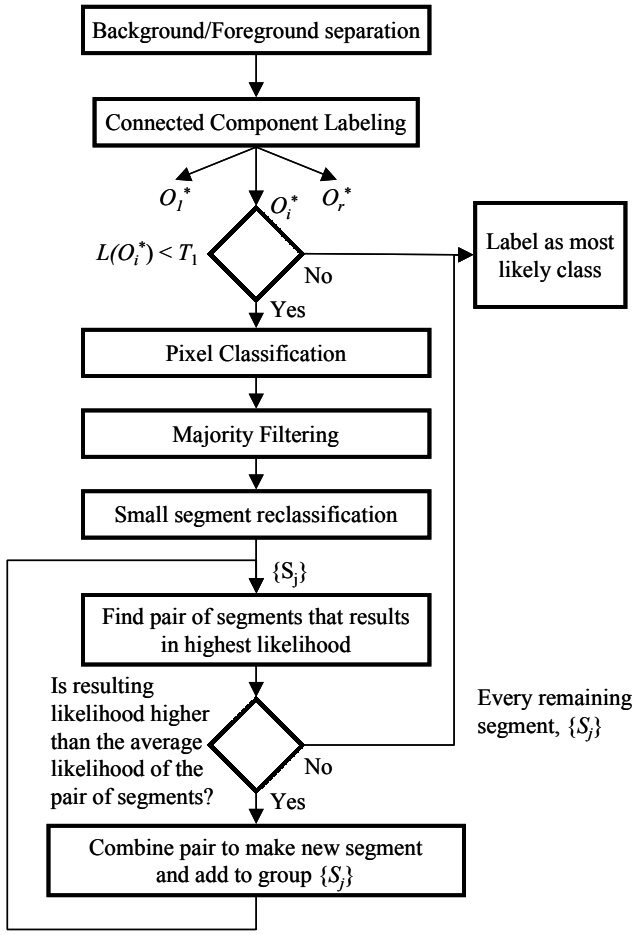

Fig. 12. Flowchart of proposed segmentation-classification algorithm.

B. Examples

Figure 13 depicts the ML joint segmentation-classification method applied to a single cluster of chromosomes. The cluster includes one touch and one overlap. Fig. 13(a) shows the original M-FISH image with hand-drawn segmentation, while Fig. 13(b) shows pixel classification using the classifier in Section III-B. The effect of the majority filter is shown in Fig. 13(c). Two small segments were reclassified: the green cluster in the upper left and a single pixel of red in the class 22 chromosome. Fig. 13(d) shows the segments after reclassification and the likelihood values of their most likely class. Fig. 13(e) shows the final segmentation likelihoods, and Fig. 13(f) shows the final classifications. The ends of the class 15 chromosome have been rejoined, as have the two segments of the class 22 chromosomes. Notice that the likelihood value of the class 12 chromosome is still low since it covers part of the class 15 chromosome.

Figure 14 shows an example of a simple image (A0105XY) segmented with the ML joint segmentation-classification method. Again pixel classification, majority filtering, and the final segmentation are shown. Here there were no segments small enough for reclassification. Small segments, in fact, are rather rare given the large size of the majority filter, but they are still possible, as witnessed in Fig. 13. In this example, two touches and the overlap were decomposed correctly.

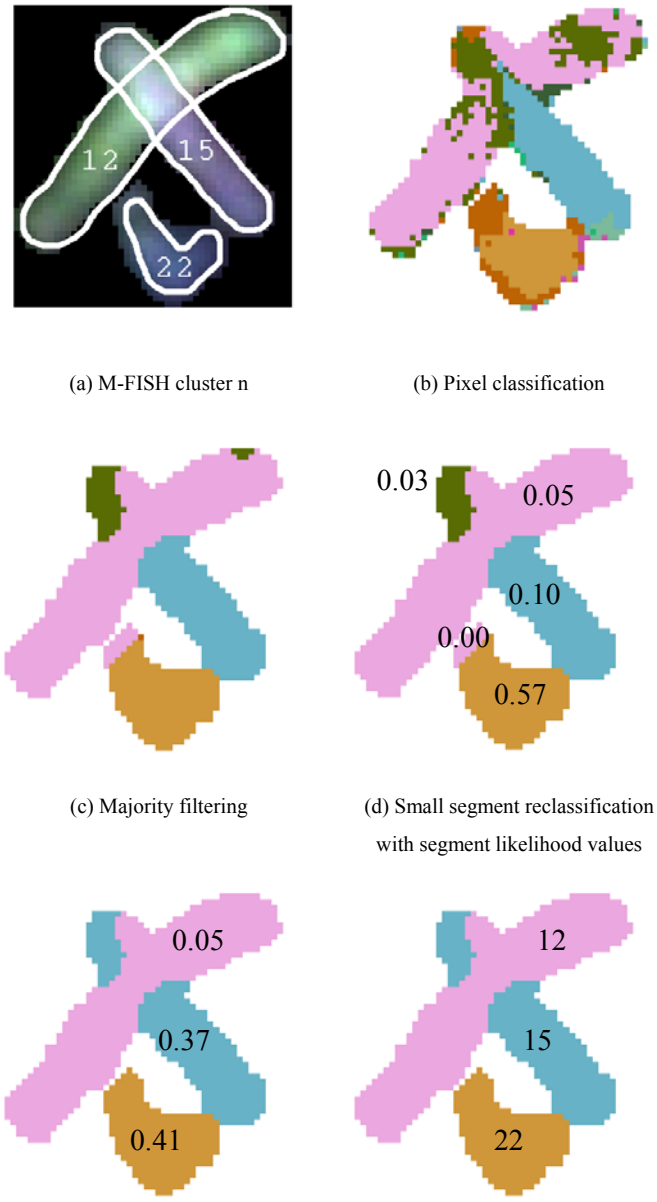

(a) M-FISH cluster n

(b) Pixel classification

(c) Majority filtering

(d) Small segment reclassification with segment likelihood values

(e) Final likelihood values

(f) Final classification

Fig. 13. Example of cluster decomposition

In Figures 15 and 16, the strengths of each method are contrasted. Figure 15 shows an example where the ML M-FISH method succeeds but grayscale methods fail. In this example, two chromosomes touch closely and are in line with each other. Using grayscale and geometric information alone, this appears to be a single chromosome, where the M-FISH multi-spectral data makes the touch clear. Fig. 16, however, is an example where multi-spectral methods fail: two chromosomes of the same class overlap. The geometric information succeeds here, but multi-spectral information does not distinguish between the two chromosomes.

While most of the examples in this section were straightforward and successfully decomposed, the ADIR M-FISH dataset includes a wide variety of images, including a number of difficult real-world images such as Fig. 16. In the next section, we discuss the algorithm performance on the whole database and examine several types of clusters which the algorithm does not segment correctly.

C. Segmentation

We compared our results with those of the popular Cytovision chromosome segmentation software [50], a commercially available chromosome imaging software package that performs grayscale image segmentation. We applied the software to the DAPI channel of each image in the ADIR chromosome image dataset. The Cytovision software is semi-automatic. It first decomposes what it believes are certain touches, then marks what it believes to be more possible clusters, and the user manually selects the touches and overlaps. It then attempts to decompose the touches and overlaps that the user selects. For comparison, we manually selected all touches and overlaps, to see what percentage are correctly decomposed. If a touch or overlap is segmented incorrectly, we left it unsegmented, rather than let it be segmented incorrectly. For this reason, the Cytovision grayscale software has many more clusters unsegmented than segmented incorrectly. If a cluster contained both touches and overlaps, we manually selected the order of decomposition that resulted in the best segmentation.

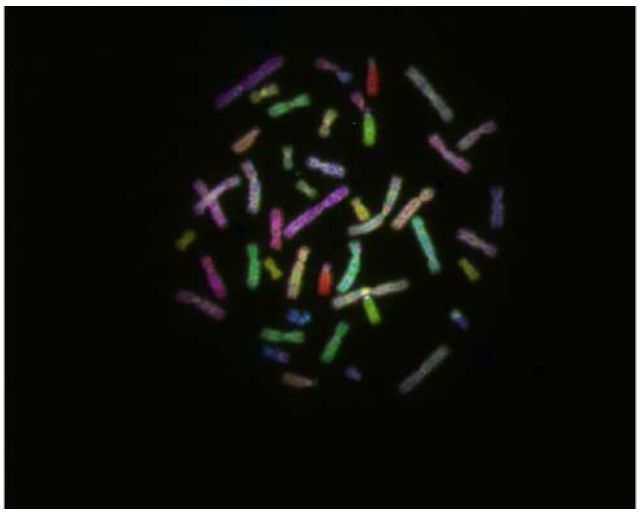

(a) M-FISH image

(c) Majority filter

(b) Pixel classification

(d) Final segmentation-classification

Fig. 14. Example of M-FISH image segmentation

The ML method runs completely automatically. It attempts to recognize all clusters and decompose them, treating touches no differently than overlaps, since they are both decomposed in the same way in the algorithm.

Since we have not concerned ourselves with background/foreground separation in this work, we assume ideal separation. For the Cytovision grayscale software, we manually selected the threshold giving the best segmentation accuracy. Cell nuclei and debris were removed manually. For the ML algorithm, we used the background/foreground separation included in the hand-segmented K file of the M-FISH image dataset. If these two different methods resulted in different clusters, those clusters were discarded, and only matching clusters were compared.

Since the Cytovison grayscale software requires human assistance, a comparison between it and the ML method might not be completely fair. For instance, very few clusters are oversegmented or missegmented in the grayscale software since the user only selects decompositions that are performed correctly. The only oversegmented and

incorrectly segmented clusters result from the software automatically segmenting clusters it believes to be obvious. To account for some of this, we have calculated the percentage of clusters and single chromosomes that both methods have identified as clusters.

The segmentation results are shown in Table II. The ML method correctly decomposed a much higher percentage of touches compared to the grayscale segmentation. The grayscale segmentation particularly has a difficult time with "hard" touches, or partial overlaps (Fig. 17), and with large clusters of many tightly packed chromosomes. Neither does very well with overlaps, although the grayscale method seems more reliable than the ML classification-segmentation. This is partly because the probabilistic modeling resists overlaps since it is uncertain about the part being overlapped. It often mistakes overlaps for a touches.

Most chromosomes incorrectly segmented by our algorithm fall into one of 5 classes:

1) The most obvious class is the example shown in Fig. 16. If two chromosomes of the same class touch or overlap, there is no way to determine their boundary with multi-spectral information alone. Grayscale or geometric information must be used in this case.

2) In certain instances a chromosome or cluster of chromosomes was incorrectly segmented because of poor background/foreground segmentation. As mentioned, we did not perform our own background/foreground segmentation, but instead use the background/foreground segmentation that was contained in the K files of the M-FISH image dataset. While the segmentation in the K files always contains the chromosomes, it does not necessarily guarantee that the masks will exactly match the border of the

(a) M-FISH image (b) ML segmentation-classification

Fig. 15. Multi-spectral methods work, but grayscale methods do not.

(a) M-FISH image (b) Grayscale segmentation

Fig. 16. Grayscale methods work, but multi-spectral methods do not.

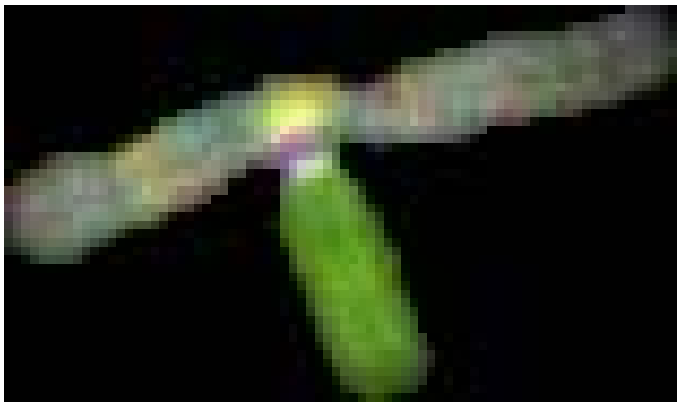

Fig. 17. "Hard" touch. Only the tip of a chromosome is overlapped, so unlike the typical overlap case, both ends of the chromosome are not visible.

TABLE II

PERCENTAGE OF CORRECT SEGMENTATION FOR VARIOUS CLUSTER TYPES

	Count	ML Method	Grayscale
Touches	720	77%	58%
Overlaps	189	34%	44%
Singles Oversegmented	3102	0.8%	0.2%

The proposed ML method is completely automatic and works on the color image, whereas the grayscale method requires human intervention

chromosomes. The masks can be larger than the chromosomes, sometimes twice as large as the chromosomes they contain. Because the likelihood value is a function of size, incorrect size information derived from the background/foreground segmentation can lead to erroneous results. Figure 18 shows the border of the K files background/foreground segmentation in white. The border hugs tightly to the edge of the chromosomes in most instances, but the bottom half of the green chromosome was manually enlarged by the dataset's creators to include the telemere.

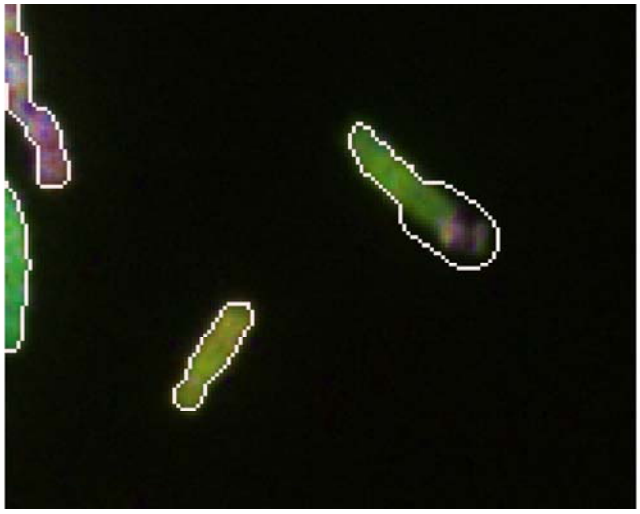

Fig. 18. Background/foreground inaccuracies in K files

3) Segmentation-classification accuracy is inherently dependent on pixel classification accuracy. Pixel classification rates vary widely throughout the M-FISH image dataset. Average pixel classification accuracy for our classifier was 68% with a standard deviation of 17.5%. Accuracies above 90% were not uncommon for some images, and some images only had pixel classification accuracies of 20-30%, or even less in a few rare cases. Fig. 20 illustrates the relationship between segmentation-classification accuracy vs. pixel classification accuracy. The "10-20" bar is statistically insignificant because there are only a few images in this group.

4) Finally, a common cause of errors in segmentation-classification was the "greedy" approach to the algorithm. The algorithm does not guarantee an optimal combination of segments in the sense of likelihood values. Instead it is a greedy algorithm, in that it only rejoins the pair that results in the highest likelihood value for a single combination. It is possible that rejoining two segments with a lower rejoined likelihood value may lead to a series of rejoinings having a higher likelihood value. In Fig. 19, the pair of segments that

TABLE III

OBJECTS RECOGNIZED AS CLUSTERS

	Count	ML Method	Grayscale
Clusters	496	95%	69%
Singles	3102	6%	0.4%

ML method recognizes more clusters, but also incorrectly recognizes more single chromosomes as clusters. However, the ML method only actually oversegments 0.8% of single chromosomes compared to 0.2% for the Cytovision method.

TABLE IV

CHROMOSOME MISCLASSIFICATION RATES

	Joint Segmentation-Classification	Only Pixel Classification
Singles	8.1%	15%

Using the proposed likelihood function for classification reduces misclassifications by nearly 50% compared to classification using only multi-spectral data.

TABLE V

ABNORMALITY DETECTION CHARACTERISTICS ON V29 IMAGE SET IN THE ADIR M-FISH DATASET

	Normal Chromosomes	Translocations	Fragments
Likelihood average	0.44	0.12	0.02
Likelihood standard deviation	0.24	0.10	0.02
< 0.1 likelihood	4.9%	50%	100%
< 0.3 likelihood	34%	96%	100%

On average the likelihood value for a translocation is significantly lower than the value for normal chromosomes.

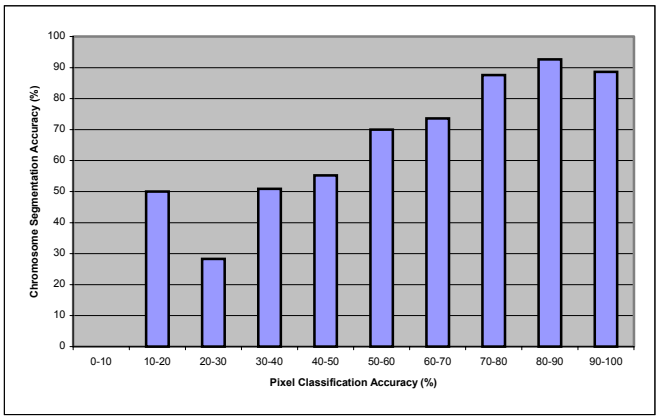

Fig. 20. Impact of pixel classification on segmentation

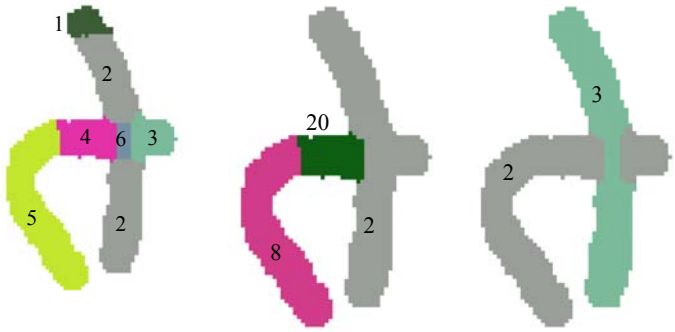

(a) Numbered segments (not classes)

(b) Average likelihood of greedy segmentation: 0.08

(c) Average likelihood of optimal segmentation: 0.28

Fig. 19. Greedy vs. optimal

results in the highest likelihood value is segments 2 and 3. Segment 3 produces a higher likelihood value than 1 and 6 since it is larger and makes the chromosome closer to its expected size for a class 3 chromosome. Also it includes some of the class 3 chromosome, so its multi-spectral information might also partially match. However, while one segment of high probability is found, there is no combination for segments 4 and 5 that results in a high probability, so the average likelihood value is low. One possible area of future improvement might be to implement a stochastic approach to combine segments.

In addition to decomposition accuracy, another important factor to consider is an algorithm's accuracy in detecting clusters, so that it will know which objects it should keep as single chromosomes and which ones it should attempt to decompose into parts. One can see in Table III that the probabilistic model recognizes a much higher percentage of clusters, but as a result also recognizes more single chromosomes as clusters. However, even though the probabilistic model recognizes 6% of singles as possible clusters, less than 1% of them are actually oversegmented when they should not have been (Table II). Very rarely will any segments within a single chromosome result in a higher probability than the chromosome as a whole. In this test, we used a threshold of a 0.1 likelihood value for determining whether a connected component or not; if a segment has less than a 0.1 likelihood value of belonging to its most likely class, we assumed that that object was a cluster or an abnormality.

D. Classification

Classification accuracy was also run on the entire 200-image ADIR M-FISH database. All chromosomes correctly segmented by the ML method were examined, both in clusters of touching and overlapping chromosomes and by themselves. Incorrect segmentations, translocations, and other abnormalities were not considered. The K files were used to determine classification accuracy. Table IV shows the misclassification rate using pixel classification. Pixel classification was done by assigning each chromosome to the class occuring most often in the classified pixels within that chromosome. The misclassification rate is nearly twice that of the proposed likelihood function $L(\cdot)$ and the joint segmentation-classification algorithm.

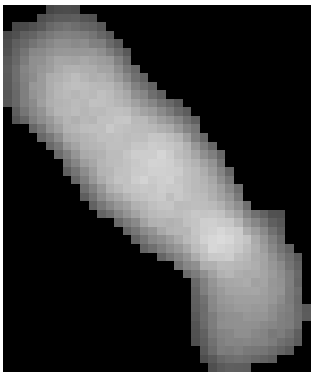

a) Grayscale

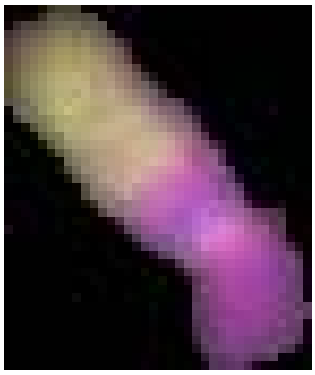

b) M-FISH

Fig. 21. t(20;5) translocation. An exchange of material between a type 20 and type 5 chromosome.

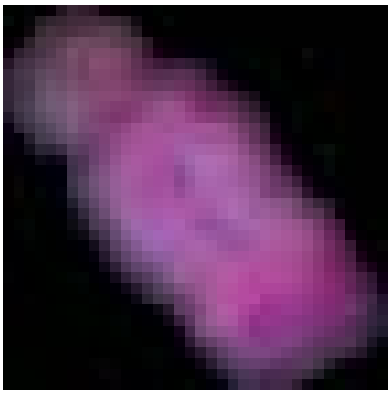

Fig. 22. Small translocation; t(7;8).

E. Chromosome Flagging

One advantage of the ML joint segmentation-classification algorithm is that the final result is a likelihood value for each chromosome segment. This value is a measure of the certainty of the classification of that segment, which is useful since it allows segments of low likelihood values to be flagged as segments requiring manual inspection.

There are four possibilities that would result in a segment of low probability:

1) The segment is a translocation, broken chromosome, or other abnormal chromosome. There is no "correct" segmentation, since the chromosome will have a low likelihood of being a chromosome, and the sections of a translocation will be too small to receive a high likelihood value.

2) The segment is incorrectly segmented. If the ML method errs and cannot find the correct segment, the resulting segments often will have low likelihood values.

3) The segment is misclassified. Even if segmented correctly, noise, weak dyes, or other factors could cause the segment to be misclassified. In this case, the likelihood value will also be low since likelihood function $L_1(\cdot)$, which measures pixel classification certainty, will be low.

4) It is possible that the segment is segmented and classified correctly, but the segment still has low likelihood value. This may also be due to noise, weak dyes, image distortion, misregistration of spectral images, etc.

In the first 3 of these 4 cases, it is useful to flag these segments so that the user can either repair the segmentation-classification error or further inspect the abnormal chromosome. In practice, all karyotypes are reviewed manually, but flagging of segments by likelihood values would certainly save time, since the user is automatically directed to the questionable segments, rather than having to examine every segment for correctness without any prior knowledge. We briefly consider each case in turn.

1) Aberration Scoring - The most important aspect of karyotyping is anomaly detection. Extra chromosomes, missing chromosomes, and translocations indicate radiation damage, cancer, and various genetic disorders. The multi-spectral data in M-FISH images make anomalies readily apparent [44]. Figure 21 is an example of a t(20:5)

(designating translocations between type 20 and type 5 chromosomes [7]). The translocation is highly visible owing to the color differential between the two sections; the grayscale version appears as a normal chromosome.

The proposed probabilistic model for segmentation-classification also aids in locating and measuring the severity of translocations, abnormalities and broken chromosomes, since their segments have low probabilities. The karyotype of such segments can then be marked as abnormal for later examination by an expert. Discovering an abnormal number of chromosomes would require incorporating chromosome count into the likelihood function; however, it is a simple matter to flag a class if it has more (or less) than its normal number of chromosomes assigned to it.

TABLE VI
LIKELIHOOD FUNCTION < 0.1

	Count	Flagged
Abnormals	114	49.1%
Incorrect Segmentation	409	52.6%
Incorrect Classification	315	48.6%
Correct Segments	3866	6.4%

The proposed likelihood function is much more likely to flag abnormals and errors in segmentation and classification than normal, correctly identified chromosomes.

Some translocations are difficult to detect, even for an expert, since they are very small. A tiny change in color at a chromosome tip may be due to noise, staining, or an actual translocation. Several images may be needed to verify that a chromosome contains a translocation. Figure 22 shows a translocation that is quite similar to a class 8 chromosome. It is much less noticeable than the translocation in Fig. 21 since it only has a very small section of class 7 chromosome, and is similar in size to a class 8 chromosome.

The proposed likelihood function also can have difficulty in detecting these small translocations since they change the size of the chromosome by only a small amount, and because there is still high confidence of the class throughout most of the chromosome. The proposed likelihood function is quite reliable, though, in detecting larger translocations and smaller than normal chromosomes that might result from a break.

Table V shows the results of running the algorithm on image set V29 from the ADIR dataset. This dataset has 15 images with 5 translocations in each, as well as some short chromosome fragments. In this test the likelihood values of the normal, correctly segmented chromosomes were compared to the likelihood values of abnormal chromosome material, the translocations and the fragmented chromosomes. Clearly, the likelihood is effective as a feature for distinguishing between normal and abnormal chromosomes. The average likelihood values of the translocations and the partial chromosomes are much lower than the average probabilities of whole chromosomes. This table also shows what percentage of normal and abnormal chromosomes were flagged with a likelihood value threshold of 0.1 - an arbitrary number used only to illustrate the disparity between the percentages of normal and abnormal chromosomes flagged. Since the average likelihood value for a translocation is 0.12, a higher threshold of 0.3 was also included, which flagged nearly all the abnormal chromosomes, but also caught more normal chromosomes. Table VI shows the results of abnormality detection on the entire database. With a likelihood value threshold of 0.1, 49.1% of the abnormal chromosomes were flagged.

(a) M-FISH cluster (b) Incorrect segmentation and classification (c) Correct segmentation and classification

Fig. 23. Single flagged segment can correct a whole cluster. Cluster is incorrectly segmented and classified. However, flagging only one segment can direct a user to correct the whole cluster.

2) Incorrect Segments - When it were not possible for an algorithm to find a correct segmentation, it is desirable that the questionable segments be flagged for human inspection. The ML algorithm makes this possible: if the ML function cannot find a likely segmentation, it results in a low likelihood value and the segments involved are easily located.

Table VI shows the percentage of incorrect segments that were flagged using a threshold of 0.1. While only 52.6% of incorrect segments are flagged, the algorithm is more effective than this number indicates, since many of the cases are part of an incorrectly segmented, multiple chromosome cluster. So while only one segment in that cluster might be flagged, this is effectively the same as flagging the cluster, since fixing that segment will likely fix other segments in that cluster that might not have been flagged. Figure 23 exemplifies this: Fig. 23(b) shows an incorrectly segmented and classified cluster. If segment 14 or 21 were the only segment flagged, they would result in the whole cluster being corrected; one cannot be fixed without the other since they are part of the same chromosome. Since the correct chromosome, 12, would then be correctly segmented, the remaining part of the cluster, the class 14 chromosome, would also be corrected.

3) Misclassifications - Misclassifications also result in low likelihood values, because they result from uncertainty caused by noise or weak labeling. Very rarely is a chromosome misclassified with a high probability. Table VI shows that likelihood is, in fact, a good indicator of misclassified chromosomes, with 48.6% of misclassified chromosomes having a likelihood value of less than 0.1. As in the case of abnormal chromosomes, the algorithm will flag a higher percentage of chromosomes if the likelihood value threshold were raised, but it would also flag a higher percentage of correct chromosomes. This might be desirable if one were willing to sort through more correct segments in order to catch more incorrect or abnormal ones. However, the arbitrary threshold of 0.1 used here amply illustrates the disparity of flagging between abnormal chromosomes and incorrect segments as compared to correct segments.

4) Correct Segments - We also include the rates for correct segments for comparison. As Table VI shows, only 6.4% of correctly segmented and classified chromosomes are flagged; correct segments only constitute 38% of the flagged chromosomes, even though there are almost 5 times as many correct segments than abnormal chromosomes, incorrectly segmented chromosomes, and misclassified chromosomes put together.

F. Complexity

The lengthiest part of the algorithm is, by far, the pixel classification, requiring, at each pixel, evaluation of a multi-dimensional Gaussian for each class and the probability that it belongs to each class. There are 5 dyes, so a 5-element mean vector multiplies a 5×5 covariance matrix and this by another 5-element mean vector, followed by a

scalar exponential: a total of 30 multiplications and 24 additions for each pixel and class. Since there are 24 classes, and the image size used is 517×645, there are nearly 240 million multiplications/additions for each image. For a typical 517×645 image, the code takes around 2.5 minutes on a 167 MHz Sun workstation to accomplish both segmentation and classification. Most of that time is used for pixel classification and probability calculation. A portion of that time is used for calculating side information not strictly necessary for the operation of the algorithm. All the code presented here is available at:
http://signal.ece.utexas.edu/~wade/mfish.

VI. Conclusion

A maximum likelihood method to segment and classify M-FISH chromosomes images using multi-spectral data was introduced. It uses pixel classification and a probabilistic model of chromosome features to select from among a set of segmentation possibilities. Segmentation and classification can be achieved simultaneously, since the model is a function of both. The method decomposes both overlaps and clusters composed of more than two chromosomes. Since the method is not specific to the characteristics of chromosomes, it could be used for other multi-spectral segmentation problems.

References

[1] M.R. Speicher, S.G. Ballard, and D.C. Ward, "Karyotyping Human Chromosomes by Combinatorial Multi-fluor FISH," Nature Genetics, vol. 12, pp. 368-375, 1996.

[2] A.M. Vossepoel, *Analysis of Image Segmentation for Automated Chromosome Identification*, University of Leiden, Leiden, Netherlands, Doctoral Dissertation, 1987.

[3] Human Chromosome Study Group, "A Proposed Standard of Nomenclature of Human Mitotic Chromosomes," *Cerebral Palsy Bulletin*, vol. 2, no. 3, 1960.

[4] M. Seabright, "A Rapid Banding Technique for Human Chromosomes," *Lancet* ii, pp. 971-2, 1971.

[5] A. T. Sumner, H. J. Evans, and R. A. Buckland, "New Techniques for Distinguishing Between Human Chromosomes," *Nature New Biology*, vol. 232, no. 27, pp. 31-32, 1971.

[6] P.C. Nowell and D.A. Hungerford, "A Minute Chromosome in Human Chronic Granulocytic Leukemia," *Science*, 132, pp. 1197, 1960.

[7] ISCN (1995): *An International System for Human Cytogenetic Nomenclature*, Mitelman, F (ed); S. Karger, Basel, 1995.

[8] J. W. Gray and D. Pinkel, "Molecular Cytogenetics in Human Cancer Diagnosis," *Cancer*, vol. 69, pp. 1536-1542, 1992.

[9] R.S. Ledley, F.H. Ruddle, J.B. Wilson, M. Belson, and J. Albarran. "The Case of Touching and Overlapping Chromosomes." In G.C. Cheng, *et al.,* (eds), *Pictorial Pattern Recognition*, Thompson, Washington DC, 1968, pp. 87-97.

[10] K. R. Castleman. "Match Recognition in Chromosome Band Structure," *Biomed. Sci. Instrum.*, vol. 4, pp. 256-64, 1968.

[11] S. Kahan, T. Pavlidis, and H. S. Baird, "On the Recognition of Printed Characters of any Font and Size," *IEEE Trans. Pattern Analysis and Machine Intelligence*, vol. 9, no. 2, pp. 274-288, 1987.

[12] B. Lerner, H. Guterman and I. Dinstein, "A Classification-Driven Partially Occluded Object Segmentation (CPOOS) Method with Application to Chromosome Analysis," *IEEE Trans. on Signal Processing*, vol. 46, no. 10, pp. 2841-2847, 1998.

[13] G. Martin, "Centered-Object Integrated Segmentation and Recognition of Overlapping Handprinted Characters," *Neural Computation*, vol. 5, no. 3, pp. 419-429, 1993.

[14] Y.W. Teh, *Learning to Parse Images*, University of Toronto, Toronto, Canada, Masters Thesis, 2000.

[15] S. MacLane and G. Birkoff, *Algebra*. Macmillan, 1979.

[16] G. Agam and I. Dinstein, "Geometric Separation of Partially Overlapping Nonrigid Objects Applied to Automatic Chromosome Classification," *IEEE Trans. Pattern Anal. Machine Intell.*, vol. 19, no. 11, pp. 1212-1222, 1997.

[17] J. Graham, "Resolution of Composites in Interactive Karyotyping," in *Automation of Cytogenetics*, 191-203, Springer-Verlag, Berlin, 1989.

[18] J. Serra, *Image Analysis and Mathematical Morphology*, Academic Press, London, 1982.

[19] J. M. Chassery and C. Gaybay, "An Iterative Segmentation Method Based on a Contextual Color and Shape Criterion," *IEEE Trans. Pattern Anal. Machine Intell.*, vol. 6, pp. 794-800, 1984.

[20] C. Garbay, "Image Structure Representation and Processing: A Discussion of Some Segmentation Methods in Cytology," *IEEE Trans. Pattern Anal. Machine Intell.*, vol. 8, pp. 140-146, 1986.

[21] L. Vanderheydt, F. Dom, A. Oosterlinck, and H. Van Den Berghe, "Two-Dimensional Shape Decomposition Using Fuzzy Subset Theory Applied to Automated Chromosome Analysis," *Pattern Recognition*, vol. 13, no. 2, pp. 147-157, 1981.

[22] Q. Wu, *Automated Identification of Human Chromosomes as an Exercise in Building Intelligent Image Recognition Systems*, Catholic University of Leuven, Leuven, Belgium, Doctoral Dissertation, 1987.

[23] L. Ji, "Intelligent Splitting in the Chromosome Domain," *Pattern Recognition*, vol. 22, no. 5, pp. 519-532, 1989.

[24] C. Arcelli and G.S. Di Baja, "A Width-independent Fast Thinning Algorithm", *IEEE Trans. Pattern Anal. Machine Intell.* vol. 7, no. 4, pp. 455-464, 1985.

[25] B. Lerner, H. Guterman, I. Dinstein, and Y. Romem, "Medial Axis Transform Based Features and a Neural Network for Human Chromosome Classification," *Pattern Recognition*, vol. 28, no. 11, pp. 1673-1683, 1995.

[26] A. Moller, H. Nilsson, T. Caspersson, and G. Lomakka, "Identification of Human Chromosome Regions by Aid of Computerized Pattern Analysis," *Exp. Cell. Res*., vol. 70, no. 2, pp. 475-478, 1970.

[27] E. Granum, T. Gerdes, and C. Lundsteen, "Simple Weighted Density Distributions, WDDs for Discrimination between G-Banded Chromosomes," *Proc. Eur. Chrom. Anal. Workshop*, Edinburgh, Scotland, 1981.

[28] F.C.A. Groen, T.K. ten Kate, A.W.M. Smeulders, and I. T. Young, "Human Chromosome Classification Based on Local Band Descriptors," *Pattern Recognition Letters*, vol. 9, no. 3, pp. 211-222, 1989.

[29] J. Gregor and E. Granum, "Finding Chromosome Centromeres Using Band Pattern Information," *Comput. Biol. Med*., vol. 21, no. 1-2, pp. 55-67, 1991.

[30] W.P. Sweeney, M.T. Musavi, and J.N. Guigi, "Classification of Chromosomes Using a Probabilistic Neural Network," *Cytometry*, vol. 16, pp. 17-24, 1994.

[31] P.A. Errington and J. Graham, "Application of Artificial Neural Networks to Chromosome Classification," *Cytometry*, vol. 14, pp. 627-639, 1993.

[32] B. Lerner, "Toward a Completely Automatic Neural-Network-Based Human Chromosome Analysis," *IEEE Trans. Trans. Systems, Man, and Cybernetics, Part B*, vol. 28, no. 4, pp. 544-552, 1998.

[33] S.O. Zimmerman, D.A. Johnston, F.E. Arrighi, M.E. Rupp, "Automated Homologue Matching of Human G-Banded Chromosomes," *Comput. Biol. Med*., vol. 16, no. 3, pp. 223-233, 1986.

[34] R.J. Stanley, J.M. Keller, P. Gader, and C.W. Caldwell, "Data-Driven Homogue Matching for Chromosome Identification," *IEEE Trans. Medical Imaging*, vol. 17, no. 3, pp. 451-462, 1998.

[35] L. Vanderheydt, A. Oosterlinck, J. Van Daele, and H. Van Den Berghe, "Design of Graph-Representation and a Fuzzy-Classifier for Human Chromosomes," *Pattern Recognition*, vol. 12, pp. 201-210, 1980.

[36] A. Carothers and J. Piper, "Computer-Aided Classification of Human Chromosomes: A Review," *Statistics and Computing*, vol. 4, no. 3, pp. 161-171, 1994.

[37] C. Lundsteen and J. Piper, *Automation of Cytogenetics*, Berlin, Springer-Verlag, 1989.

[38] D. Pinkel, T. Straume, and J.W. Gray, "Cytogenetic Analysis Using Quantitative, High-sensitivity, Fluorescence Hybridization," *Proc. National Acad. of Science*, vol. 83, pp. 2934-2938, 1986.

[39] P. M. Nederlof, S. van der Flier, J. Wiegant, A. K. Raap, H. J. Tanke, J. S. Ploem, and M. van der Ploeg, "Multiple Fluorescence in Situ Hybridization," *Cytometry*, vol. 11, pp. 126-131, 1990.

[40] P. M. Nederlof, S. van der Flier, J. Vrolijk, H. J. Tanke, and A. K. Raap, "Fluorescence Ratio Measurements of Double-labeled Probes for Multiple in Situ Hybridization by Digital Imaging Microscopy," *Cytometry*, vol. 13, pp. 839-845, 1992.

[41] M. M. Le Beau, "One FISH, two FISH, red FISH, blue FISH," *Nature Genetics*, vol. 12, pp. 341-344, 1996.

[42] T. Ried, A. Baldini, T.C. Rand, and D.C. Ward, "Simultaneous Visualization of Seven Different DNA Probes by in Situ Hybridization using Combinatorial Fluorescence and Digital Imaging Microscopy," *Proc. National Acad. Science*, vol. 89, pp. 1388-1392, 1992.

[43] M. P. Sampat, K. Castleman and A. C. Bovik, "Pixel-by-Pixel Classification of M-FISH Images", *Proc. IEEE Engineering in Medicine and Biology Society and the Biomedical Engineering Society*, October 23-26, 2002, Houston, TX.

[44] T. Veldman, C. Vignon, E. Schröck, J. D. Rowley, and T. Ried, "Hidden Chromosome Abnormalities in Haematological Malignancies Detected by Multicolour Spectral Karyotyping," *Nature Genetics*, vol. 15, pp. 406-410, 1997.

[45] W. Schwartzkopf, B.L. Evans, and A.C. Bovik, "Minimum Entropy Segmentation Applied to Multi-Spectral Chromosome Images", *Proc. IEEE Int. Conf. on Image Processing*, Oct. 7-10, 2001, vol. II, pp. 865-868, Thessaloniki, Greece.

[46] W. Schwartzkopf, B.L. Evans, and A.C. Bovik, "Entropy Estimation for Segmentation of Multi-Spectral Chromosome Images", *IEEE Southwest Symposium on Image Analysis and Interpretation*, April 7-9, 2002, pp. 234-238, Santa Fe, NM.

[47] H. Stark and J. Woods, *Probability, Random Processes, and Estimation Theory for Engineers,* Prentice Hall, 1994.

[48] M. Sezgin and B. Sankur, "Survey over image thresholding techniques and quantitative performance evaluation," *Journal of Electronic Imaging*, vol. 13, pp. 146-168, 2004.

[49] http://www.adires.com/05/Project/MFISH_DB/MFISH_DB.shtml

[50] http://www.dssimage.com/cytoVision.html